J. M. A. Tanskanen, J. Mattila, M. Hall, T. O. Korhonen, and S. J. Ovaska, "Predictive closed loop transmitter power control," in *Proc. 1996 IEEE Nordic Signal Processing Symposium*, Espoo, Finland, Sept. 1996, pp. 5–8.

Predictive Closed Loop Transmitter Power Control

Jarno M. A. Tanskanen[1], Jari Mattila[2], Michael Hall[2], Timo O. Korhonen[2], and Seppo J. Ovaska[3]

[1]Helsinki University of Technology
Institute of Radio Communications
Laboratory of Signal Processing and Computer Technology
Otakaari 5 A,
FIN-02150 Espoo, Finland
E-mail: jarno.tanskanen@hut.fi

[2]Helsinki University of Technology
Institute of Radio Communications
Communications Laboratory
Otakaari 5 A,
FIN-02150 Espoo, Finland

[3]Helsinki University of Technology
Laboratory of Electric Drivers and Power Electronics
Otakaari 5 A,
FIN-02150 Espoo, Finland

ABSTRACT

In this paper, a predictive closed power control loop for mobile communication systems is simulated. The system parameters are derived from those used in a CDMA system uplink transmission at urban mobile speeds. This presents no restrictions, however, on using the proposed method in any closed loop control system where the total received power level is to be estimated from noisy measurements. It is shown by COSSAP (*Communications Simulation and System Analysis Program of CADIS GmbH, Germany*) *simulations that when the estimates of the received power level are noisy, and the control loop response is inherently delay-limited, predictive lowpass filtering can be applied to improve the received power level estimates and overall system performance. This method yields better tracking of Rayleigh fading, and improved bit-error-rates* (*BER*)*, as compared to those achieved with a non-predictive reference controller.*

1. INTRODUCTION

As the CDMA systems are inherently interference limited, it is of paramount importance to keep the transmission power of each mobile user as low as possible [1]. This is crucial in the uplink transmission (from mobile to base station), where all the mobile units need to be controlled by the base station to keep the *received power level* from each mobile unit constant in the average. The need for power control has been widely studied, and the capacity of a CDMA system is found to greatly depend on the power control function [1], [2]. In this study, the mobile transmitter power control, used to compensate for the effects of Rayleigh fading, is achieved through a closed power control loop for which it is necessary to estimate the received power level.

The function of predictive filtering is twofold: to predict future values of the power signal, and to reduce the additive noise and interferences corrupting the power signal. An additional requirement in a control application like this is that the control loop should remain *stable* in all conditions; this sets explicit requirements for the predictive filter as well.

In the system described in this paper, the control is based on the noisy total received power level, and a single user single path propagation case is investigated. Because the control function is based on the total received power, and not on the received power as per user, the simulated control strategy is applicable only to single user systems. Still, our results clearly demonstrate the achievable benefits of predictive lowpass filtering of received power level estimates within a closed control loop.

The simulator is described in detail in Section 2. The simulation results are given in Section 3, and the main benefits are shortly summarized in Section 4.

2. THE SIMULATOR

To clearly demonstrate the effects of the predictive power controller, other simulator components are kept as simple as possible. Thus, no corrective coding nor interleaving is used, for example. The simulation is performed in complex lowpass equivalent signal domain, and the simulation parameters are derived from those presented for the Qualcomm CDMA system in [3]. Some sampling time scaling is necessary to ensure statistical properties of the signals, and also certain parameters are adjusted to allow for realizable simulation execution times. Data is a pseudo random binary sequence produced by a maximum length shift register with period $2^{31}-1$. In this simulator, the only effect of the spreading is to provide code gain, and so to reduce simulation execution time the spreading code is set to all ones, i.e., omitted. While the Qualcomm system uses 128 chips per bit [3], our simulator uses 127 chips per bit to allow also spreading code generation by a maximum length shift register with period 127. The simulator runs at the chip frequency of 1.2288 MHz as in [3]. This is also the sampling rate used. The applied Rayleigh fading generator was noticed to produce unsatisfactory Rayleigh fading characteristics at urban mobile speeds if sampled at 1.2288 MHz. In order to ensure correct statistics, the Rayleigh fading is sampled at $1.2288\ \text{MHz} / 16 = 76800\ \text{Hz}$. From this it follows that in order to maintain the desired fading rate per chip, the mobile speed must also be scaled down by 16, and 16 times more samples are needed to simulate a desired time period. The overall result is naturally the same as if the Rayleigh fading was sampled at 1.2288 MHz. To

clarify the power control effects, and to reduce simulation execution time, the power control frequency is double that given in [3]. In our simulator, transmission power is controlled every six bits, resulting in a power control interval of approximately 0.6 ms. At each control instant, the transmission power is either increased or reduced by 1 dB, which is also one of the possible settings in the Qualcomm system [3]. The control loop delay, including all processing and propagation delays, is set to one chip duration. The overall simulator is depicted in Fig. 1. Additive white Gaussian noise (AWGN) is used to model the receiver noise and any possible interferences.

2.1. Transmitter Model

The transmitter applies differential encoding and binary phase shift keying to the data. The operations are denoted together as 2DPSK. Regardless of the complex baseband simulation environment, the transmitted signal is thus always real. The transmitter power is set by multiplying the chip sequence by a power control multiplier $p(n)$, later also referred to as the transmitter power setting. n is the sample index at chip rate. Nominally, the powers of both in-phase and quadrature components are set to unity.

After each power control interval, a new power control multiplier is calculated according to the previous power control multiplier and the power control bit B_c received from the power controller in the base station. Subscript c is the control period index. When the received power control bit is "1", the previous transmitter power control multiplier is decremented by -1 dB, and in the case of a power control bit "0", incremented by +1 dB:

$$p_c(n) = \begin{cases} p_{c-1}(n-1) \cdot 10^{-1/20}, & \text{when } B_c = 1 \\ p_{c-1}(n-1) \cdot 10^{1/20}, & \text{when } B_c = 0 \end{cases} \qquad (1)$$

with $p(n)$ within the limits

$$\left(10^{-1/20}\right)^{15} \le p(n) \le \left(10^{1/20}\right)^{15}, \qquad (2)$$

i.e., the overall dynamic range is set to ±15 dB from the nominal transmitter level. In the beginning of the transmission, the transmission level is set to $p(0) = -15$ dB from the nominal transmission level. In the transmitter, the transmitter power setting is monitored.

2.2. Radio Channel Model

In the channel, Rayleigh fading, generated by appropriately shaping noise [4], is applied to the transmitted signal. The average fading power is set to 0 dB, and the width of the fading spectrum is set according to the mobile speed. Additive white Gaussian noise (AWGN) is added to simulate receiver noise and interferences. In the radio channel model, the fading power is monitored.

2.3. Receiver Model

We assume perfect synchronization at the receiver. The received signal is integrated over the bit period, and 2DPSK decoding is applied. The decoder makes decisions based on the Euclidean distances in the complex symbol space. The achieved bit error rate is recorded using the knowledge of the actual transmitted data. From the receiver, the total received complex signal is fed to the controller as the input.

2.4. Power Controller Model

The power control is based on the estimated total received signal power. The controller aims to maintain the desired received power level. In the controller, the effects of the transmitter power setting to the received signal level have to be removed before the prediction can be applied. This is done by dividing the received in-phase and quadrature components, $x_i(n)$ and $x_q(n)$, respectively, by the mobile power setting $p(n)$ to obtain a predictable, smoothly changing but noisy channel power response. Four different prediction schemes are considered: The prediction is applied either a) to the received in-phase and quadrature components independently, or b) to the sum of squared components, both at the chip rate, or, b) to the average power of the components calculated independently over the control period, or d) to the average sum of squares of the components. Thus, in the schemes c) and d), the predictor input is sampled at the control frequency, i.e., every 6 bits. After prediction, the transmitter power setting information is restored, and thresholding is used to generate a power control command bit to be sent to the transmitter. The powers are scaled to present average chip powers in order to be able to set the threshold to unity. The value B_c of the control command bit, send to the mobile every $C = 762$ samples, is given by

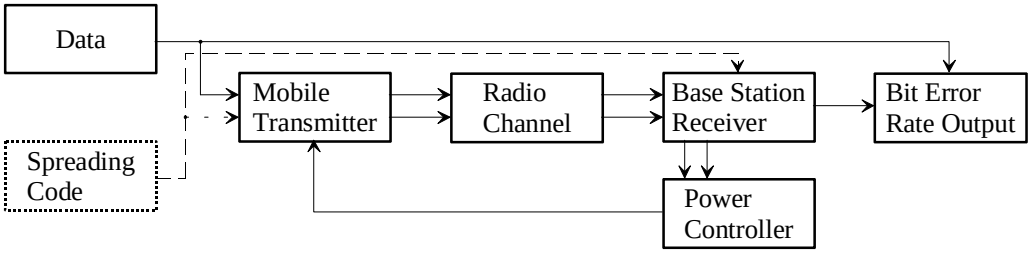

Fig. 1. Overall diagram of the power control simulator. Spreading code does not affect the controller performance.

$$B_c = \mathrm{t_c}(y_c)\text{, with } \mathrm{t_c}\left(y_c\left(n_c\right)\right) = \begin{cases} 1, & \text{when } y_c\left(n_c\right) \geq 1 \\ 0, & \text{when } y_c\left(n_c\right) < 1 \end{cases} \quad (3)$$

where n_c is the index of the last sample of the control period *c*. For the control schemes a), b), c) and d), y_c are given by (4), (5), (6) and (7), respectively, with the first degree Heinonen-Neuvo (H-N) polynomial predictor coefficients $h(1), \ldots, h(K)$ [5], here $K = 15$. Equations are written to directly correspond to the simulator block ordering. In the reference controller

$$y_c\left(n_c\right) = \frac{1}{C}\sum_{m=1}^{C}\left[x_i\left(n_c - m + 1\right)^2 + x_q\left(n_c - m + 1\right)^2\right]. \quad (8)$$

The reference controller is identical with the predictive controllers, except that the predictors are omitted. The power calculations completely eliminate the effects of data to the control. When predicting at the chip rate in case a), data causes only minor disturbances at the bit boundaries if the subsequent differentially encoded bits differ. As the predictor length is only a fraction of the bit duration in samples, these effects are negligible. Should the achieved BER be good enough, the data could be removed before prediction, but in our simulation this would introduce more errors into the fading estimate.

In future research, the control is to be based on per user received power level, or on received SNR, and actual multiuser systems are to be simulated.

2.5. The Predictor

The first degree H-N lowpass polynomial predictor [5] of length $K = 15$, analyzed in [6], is used in this study. It is to be noted that this particular predictor may not be the optimum choice for the application, but is selected for ease of implementation, and existence of optimized closed form coefficients for exact prediction of polynomial signals in white Gaussian noise [5]. From [6] it is seen that the predictor of the selected degree and length is a reasonable compromise with the simulation parameters used in that paper. Also, as FIRs, these predictors are stable but naturally this does not guarantee that the closed control loop itself would be stable. At urban mobile speeds, the Rayleigh fading can be accurately modeled as a piecewise low-degree polynomial, and the power control loop accuracy is inherently delay limited. It is also noted, that with the controller setup presented in this paper, the predictor input sampling frequency is much higher than that used in [6], resulting in more first-degree-polynomial-like behavior of the Rayleigh fading predictor input.

3. SIMULATION RESULTS

The only prediction scheme that provides performance improvements is found to be a) (4), i.e., prediction before any power calculations. Whenever prediction is done after the squaring operation, the BERs are close to those achieved with the reference controller. Figs. 2 - 5 present the main results when the controller employs prediction scheme a) (4). In each simulation, 100000 bits are simulated. The 'component SNR' axis tick label values in Figs. 4 and 5, are derived from simulated component AWGN variances 0, 0.1, …, 0.9.

In Fig. 2, at 5 km/h with component SNR 0.97 dB, both the reference and the predictive controller are fully functional and can fairly well control the channel. In Figs. 2 and 3, also the channel fading is plotted, so that the response of the controllers can be observed. The predictive controller discards some of the noise power, and thus commands for higher transmitter power, Fig. 2. This also leads to a better BER, as seen from Fig. 4 at component SNR 0.97 dB.

In Fig. 3, also at 5 km/h but under component SNR 0 dB, the reference controller operation fails. As the controller setpoint is the 0 dB power level, the reference controller assumes that its received power is sufficient for most of the time, and erroneously commands the mobile transmitter to keep the transmission power near the minimum. Also BER degrades crucially at this point, Fig. 4. The predictive controller is still able to well track the actual fading signal, Fig. 3, and is not fooled by the high noise level. Also BER degradation is only gradual, as seen in Fig. 4.

In Fig. 5, achieved BERs are shown at mobile speed 50 km/h, and the same behavior as at 5 km/h is ob-

---

a) $$y_c\left(n_c\right) = \frac{1}{C}\sum_{n=1}^{C}\left\{\left[p(n)\sum_{k=1}^{K}\frac{h(k)\cdot x_i(n-k+1)}{p(n-k+1)}\right]^2 + \left[p(n)\sum_{k=1}^{K}\frac{h(k)\cdot x_q(n-k+1)}{p(n-k+1)}\right]^2\right\} \quad (4)$$

b) $$y_c\left(n_c\right) = \frac{1}{C}\sum_{n=1}^{C}p(n)^2\sum_{k=1}^{K}h(k)\cdot\left[\left(\frac{x_i(n-k+1)}{p(n-k+1)}\right)^2 + \left(\frac{x_i(n-k+1)}{p(n-k+1)}\right)^2\right] \quad (5)$$

c) $$y_c\left(n_c\right) = p_c\left(n_c\right)^2\left\{\sum_{k=1}^{K}h(k)\frac{1}{C}\sum_{m=1}^{C}\left(\frac{x_i\left(n_c' - m + 1\right)}{p\left(n_c' - m + 1\right)}\right)^2\Bigg|_{n_c'=n_c-Ck+C} + \sum_{k=1}^{K}h(k)\frac{1}{C}\sum_{m=1}^{C}\left(\frac{x_q\left(n_c' - m + 1\right)}{p\left(n_c' - m + 1\right)}\right)^2\Bigg|_{n_c'=n_c-Ck+C}\right\} \quad (6)$$

d) $$y_c\left(n_c\right) = p_c\left(n_c\right)^2\sum_{k=1}^{K}\left\{h(k)\frac{1}{C}\sum_{m=1}^{C}\left[\left(\frac{x_i\left(n_c' - m + 1\right)}{p\left(n_c' - m + 1\right)}\right)^2 + \left(\frac{x_i\left(n_c' - m + 1\right)}{p\left(n_c' - m + 1\right)}\right)^2\right]\Bigg|_{n_c'=n_c-Ck+C}\right\} \quad (7)$$

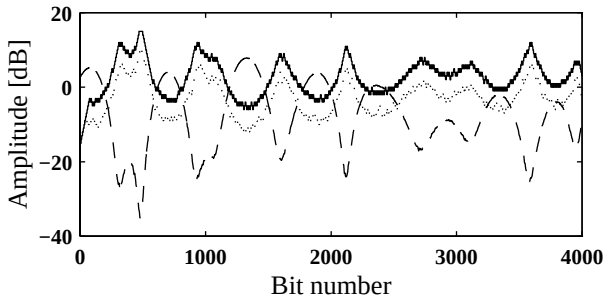

Fig. 2. Transmitter power setting in a system with (solid) and without (dotted) predictors under component SNR of 0.97 dB, along with the fading power (dashed).

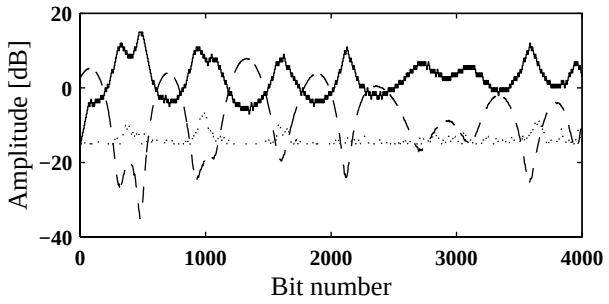

Fig. 3. Transmitter power setting in a system with (solid) and without (dotted) predictors under component SNR of 0 dB, along with the fading power (dashed).

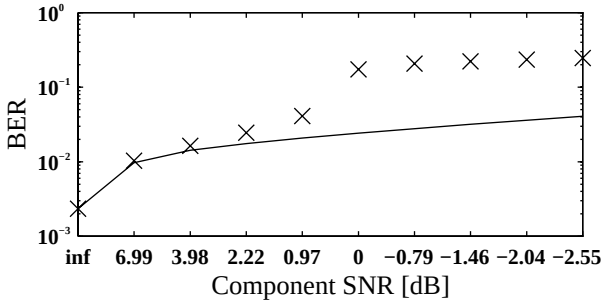

Fig. 4. BER as function of component SNR with (solid) and without (crosses) predictors within the controller at mobile speed 5 km/h.

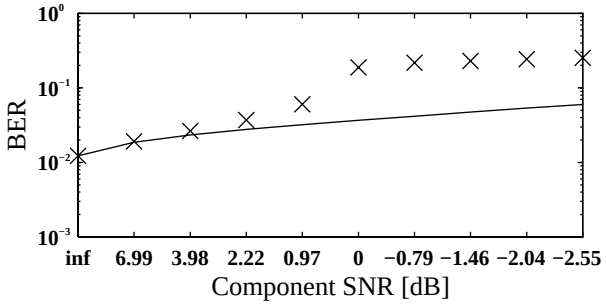

Fig. 5. BER as function of component SNR with (solid) and without (crosses) predictors within the controller at mobile speed 50 km/h.

served. The achieved BERs are somewhat worse than at 5 km/h because at this speed the controller cannot counteract all the fading.

In any case, some of the received noise power is accounted toward the setpoint, and the long term average of the actual received signal power decreases as the noise level increases. In addition to the noise itself, this also contributes to the gradual degradation of BERs, seen in Figs. 4 and 5, excluding the collapse point of the conventional controller.

4. CONCLUSIONS

In this paper, it is shown by simulations that the applied predictive lowpass filtering can be successfully used in received power level based controllers to track noisy Rayleigh fading. At high noise levels, when the conventional controller fails to function, and as a consequence the transmission also fails, the predictive controller is still able to track the actual fading, and correctly command the mobile transmitter so that also BER is still acceptable.

ACKNOWLEDGMENT

This work has been funded by the Technology Development Centre of Finland, Nokia Corporation, Telecom Finland, and Helsinki Telephone Company. The work of Jarno Tanskanen has also been supported by the Päijät-Häme Fund under the Auspices of the Finnish Cultural Foundation, and by Foundation of Technology, Finland.

REFERENCES

[1] K. S. Gilhousen, I. M. Jacobs, R. Padovani, A. J. Viterbi, L. A. Weaver, Jr., and C. E. Wheatley III, "On the capacity of a cellular CDMA system," *IEEE Trans. on Vehicular Technology*, vol. 40, pp. 303–312, May 1991.

[2] O. K. Tonguz and M. M. Wang, "Cellular CDMA networks impaired by Rayleigh fading: system performance with power control," *IEEE Trans. on Vehicular Technology*, vol. 43, pp. 515–527, Aug. 1994.

[3] "An overview of the application of code division multiple access (CDMA) to digital cellular systems and personal networks," Qualcomm, Inc., USA, 1992.

[4] M. J. Gans, "A power-spectral theory of propagation in the mobile-radio environment," *IEEE Trans. on Vehicular Technology*, vol. 21, pp. 27–38, Feb. 1972.

[5] P. Heinonen and Y. Neuvo, "FIR-median hybrid filters with predictive FIR substructures," *IEEE Trans. on Acoustics, Speech, and Signal Processing*, vol. 36, pp. 892–899, June 1988.

[6] J. M. A. Tanskanen, A. Huang, T. I. Laakso, and S. J. Ovaska, "Prediction of received signal power in CDMA cellular systems," in *Proc. 45th IEEE Vehicular Technology Conference*, Chicago, IL, July 1995, pp. 922–926.